SOME IMPROVEMENTS OF THE DATA PROCESSING ALGORITHMS IN THE TIME-OF-FLIGHT MASS-SPECTROMETRY OF HEAVY IONS

D.V. Kamanin[1], Yu.V. Pyatkov[2,1], Z.I. Goryainova[1], V.E. Zhuchko[1], A.A. Alexandrov[1], I.A. Alexandrova[1], P.Yu. Naumov[2], R. Korsten[3], V. Malaza[3], E.A. Kuznetsova[1], A.O. Strekalovsky[1], O.V. Strekalovsky[4,1]

[1]*Joint Institute for Nuclear Research, Dubna, Russia*
[2]*National Nuclear Research University MEPhI (Moscow Engineering Physics Institute), Moscow, Russia*
[3]*University of Stellenbosch, Faculty of Military Science, Military Academy, Saldanha 7395, South Africa*
[4]*Dubna State University, 141980 Dubna, Russia*

INTRODUCTION

The physical program implemented by the FOBOS group more than ten last years is dedicated to the study of different manifestations of clustering in heavy low excited nuclei [1, 2]. In the mass correlation distribution of fission fragments (FFs) from ^{252}Cf (sf) and ^{235}U(n_{th}, f) reaction a specific two-dimensional region of increased yields that is far from the loci of conventional binary fission has been revealed for the first time. In its projection onto the axis of light FFs, there are two peaks corresponding to the magic isotopes ^{68}Ni and ^{72}Ni, which is why we dubbed the region the "Ni-bump". The experimental yield of the events that make up the bump does not exceed $4\cdot10^{-3}$ per binary fission.

The Ni-bump is one of the most clear manifestations of a new type of ternary decay of heavy nuclei, called by us collinear cluster tri-partition (CCT) due to the specific features of the decay, namely the decay partners fly apart almost collinearly, and at least one of them shows magic nucleon composition.

In addition, for the first time we have observed the binary break-up of the fission fragment due to inelastic scattering in the metal foil with a thickness close to the total range of fission fragments [3]. The residual energy of the fragment does not exceed several MeV. Based on the obtained results we suppose that the fragments directly after scission of the mother system look like a di-nuclear system consisting of the magic core and the light cluster.

Four features of the processes under study essential for the experimental method to be used should be underlined: a relatively low yield of the events to be searched for (10^{-5}–10^{-3} per binary fission); a large range of the masses (4–210 u) and energies (2–110 MeV) of the decay products; very small, ~1°, open angle between the partners flying in the same direction; and short, up to a zero, time interval between the sequential hits of the PIN-diode by these fragments.

Most of the results were obtained using the "missing mass" approach which means that two decay products (fragments) are detected in coincidence in coincidence using a double armed time-of-flight (TOF) spectrometer, while the significant difference between their total mass $M_s = M_1 + M_2$ and the mass of a mother system serves as a sign of at least ternary decay. A fragment mass is calculated by the energy E and the velocity V using time-of-flight spectrometers based on the mosaics of PIN-diodes.

The use of semiconductor detectors for measuring ion's energy and for obtaining time stamp has two methodological issues that are necessary to address. First of them is the pulse-height defect (PHD) that manifests itself in a form of seemingly less energies than particles actually have. The second is the plasma delay effect (PD) that prevents precise measurement of the fragment TOF. Our experimental method provides solution of the both these problems. The method was presented in Refs [6, 7]. At the first stage, the digital images of all the detector signals are obtained using CAEN Switched Capacitor Digitizer DT5742, while all subsequent signal processing is performed off-line. The FFs mass and energy reconstruction procedure is based on the PHD parameterization proposed in Ref. [8]. To avoid the influence of the PD effect, an original time-pickoff "sewing-parabola" method proposed in Ref. [7] is used.

In this work:

- an analytical justification is given for the method of measuring the energy of a heavy ion with an arbitrary response function of the preamplifier of the PIN diode signal (previously, the correctness of the method was confirmed only empirically and only for FFs [8]);
- pulse-height defect parametrization for registration of fission fragments of PIN diode is refined;
- the results of testing the time-pickoff "sewing-parabola" method in a differential experiment are presented.

ION ENERGY SPECTROMETRY AT HIGH COUNTING RATE OF THE SPECTROMETER

In the classical approach, to estimate the charge q created by an ion in the detector volume, the area under the input current graph $i(t)$ is calculated:

$$E \sim q = \int_{-\infty}^{\infty} i(t)dt \tag{1}$$

In its turn, q is proportional to the ion energy E in the absence of PHD. In practice, it means that the current $i(t)$ is integrated with the time constant much larger than the current duration, and corresponding voltage impulse looks like a long (tens microseconds) stair-step, while time interval between the sequential hits of two CCT products of a PIN-diode could lie in the nanosecond range. For independent registration of such signals (so called "double hit" mode) they must be short shaped. In order to avoid overlap, a similar requirement for the signal duration arises when the spectrometer is operating in conditions of high counting rate.

Let us show that with an arbitrary response $h(t)$ of the spectrometric electronic circuit connected to the detector the aria of the output signal S stays proportional to the charge q. Given the linearity of the system at the output of this external circuit, a response $U(t)$ to the current $i(t)$ can be calculated as follows:

$$U(t) = \int_{0}^{t} i(r)h(t-r)dr \tag{2}$$

That is, the convolution of the function describing the input current $i(t)$ with the response function of the subsequent electronic path $h(t)$.

According to the meaning of the problem, $U(t)$ is the shape of the pulse supplied to the input of the digitizer. The area S of the pulse $U(t)$ is determined by the expression:

$$S = \int_0^\infty U(t)dt = \int_0^\infty \left\{ \int_0^t i(r)h(t-r)dr \right\} dt \quad (3)$$

This double integral could be reduced to two repeated ones (Fubini's theorem [9]):

$$S = \int_0^\infty U(t)dt = \int_0^\infty \left\{ \int_0^t i(r)h(t-r)dr \right\} dt = \int_0^\infty i(r)dr \int_r^\infty h(t-r)dt \quad (4)$$

Let us make a change of variables in the internal integral:

$$t \to z = t - r$$

Then z varies between 0–∞ and:

$$S = \int_0^\infty i(r)dr \int_r^\infty h(t-r)dt = \int_0^\infty i(r)dr \int_0^\infty h(z)dz = C \int_0^\infty i(r)dr = Cq \quad (5)$$

where C = const is the area of the response function, and q is the charge created by the fragment in the detector. The constant C is calculated during calibration using alpha particles, under the assumption that there is no PHD for them.

The algorithm for estimating the charge created by a particle in the detector by finding its area avoids the ballistic error inherent to estimating q from the pulse amplitude [10]. The ballistic error is caused by the dependence of the amplitude of the pulse on its shape for any finite constant of integration of the current pulse $i(t)$. In the presence of a plasma delay, which depends on the mass and energy of the fragment, the presence of a ballistic error is guaranteed, which determines the relevance of the approach to measure the energy of CCT products based on formula (5).

The example of registration of the FFs in the double hit mode is presented in figure 1. As can be inferred from the figure, two FFs were detected in PIN diode during 200 ns registration gate. Each fragment also hits the start detector.

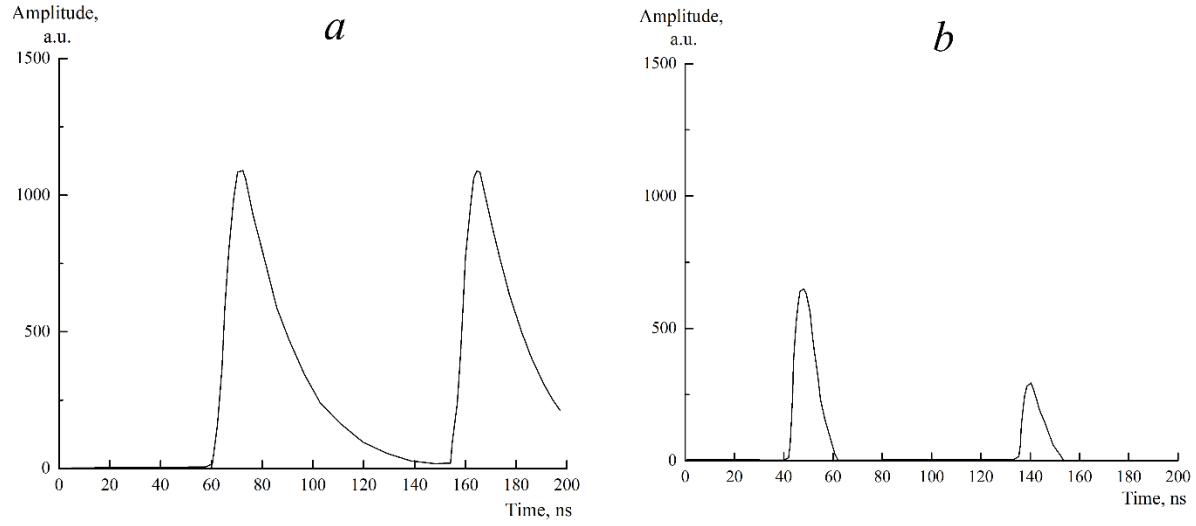

FIGURE 1. Example of registration of the FFs in the “double hit” mode. Signals from the same event at two different exits of the multichannel DT5742 digitizer are shown: *a* – signals from one of the PIN diodes of the mosaic; *b* – signals from the start detector.

MODERNIZATION OF THE PHD PARAMETRIZATION

In order to take into account the FF pulse height defect $R(M, E)$, the following parameterization was proposed in Ref. [8]:

$$R(M,E) = \frac{\lambda E}{1+\frac{\varphi E}{M^c}} + \alpha M^d E + \beta M^f E \qquad (6)$$

Here E and M are the FF energy and mass. The formula includes the vector of parameters $\{\lambda, \varphi, \alpha, \beta, c, d, f\}$. In order to determine the constants, the authors of Ref. [8] analyzed all known experimental data on $R(M, E)$ within the least squares' method (the χ^2-method) using MINUIT program [11]. They demonstrated that the minimum value of χ^2 is achieved with the power coefficients values slightly differing from the d = 1 and f = 0, and the authors recommended to use those values for the sake of significant simplification of the formula. So far, we have used the revision of the formula for $R(M,E)$ with the recommended integer values of d and f degrees:

$$R(M,E) = \frac{\lambda E}{1+\frac{\varphi E}{M^2} + \alpha ME + \beta E} \qquad (7)$$

In our FFs mass reconstruction procedure [5], the vector $\{\lambda, \varphi, \alpha, \beta\}$is calculated by fitting to the known FFs mass spectrum of ^{252}Cf(sf). Usually the parameters λ and φ are set constant, as recommended in Ref. [8], or varied slightly, up to ten percent from the initial values.

To increase the robustness of the procedure in regard to the errors of the input variables [5], an attempt was made to use a more flexible parameterization for $R(M, E)$. For this, the last two terms in Eq. (7) were changed as follows:

$$\alpha M^{(1+\Delta d)} E + \beta M^{\Delta f} E \qquad (8)$$

where Δd and Δf are corrections to the powers of d and f recommended in Ref. [8] (Eq. (6)).

TABLE. The FFs masses and velocities obtained using extended $R(M, E)$ parameterization.

PIN №	V_L, sm·ns^{-1}			V_H, sm·ns^{-1}			M_L, u		
	V_{lit}	V_{exp}	ΔV	V_{lit}	V_{exp}	ΔV	M_{exp}	M_{lit}	ΔM
1	1.34	1.32	0.02	1.003	0.988	0.015	107.25	106.6	0.65
2	1.34	1.32	0.02	1.003	0.983	0.02	107.25	106.6	0.65
3	1.34	1.316	0.024	1.003	0.983	0.02	107.25	106.4	0.85

PIN №	M_H, u			Δd	Δf
	M_{exp}	M_{lit}	ΔM		
1	141.28	141.7	-0.42	-0.35	0.47
2	141.28	141.9	-0.62	-0.69	0.49
3	141.28	140.8	0.48	-0.19	-0.15

In Table V_L, V_H, M_L, M_H are the most probable velocities and masses for the FFs of the light and heavy mass peaks of ^{252}Cf(sf) respectively; ΔV, ΔM are the differences between the values known from the literature (lit) and those obtained in experiment (exp) [12]; Δd, Δf – the power coefficients in Eq. (8).

The FFs mass reconstruction procedure similar to that described in Ref. [5] with the extended $R(M, E)$ parameterization (8) was applied to the processing of the FFs mass spectra from ^{252}Cf(sf). The results for three PIN diodes are presented in Table. As can be inferred

from the table the values of additional parameters Δd and Δf are significantly different from the previously adopted (7) values. It means that these parameters are significant for the adequate $R(M, E)$ parameterization.

VALIDATUION OF THE SEWING-PARABOLA TIMESTAMP (SPT) METHOD

The idea of the SPT method is as follows. We search for the parabolic approximation of the initial part of the PIN diode signal under conditions that the parabola vortex lies on the mean value of the pulse's baseline, while parabolic and linear parts of the leading edge (figure 2) would sew together seamlessly (see [7] for details).

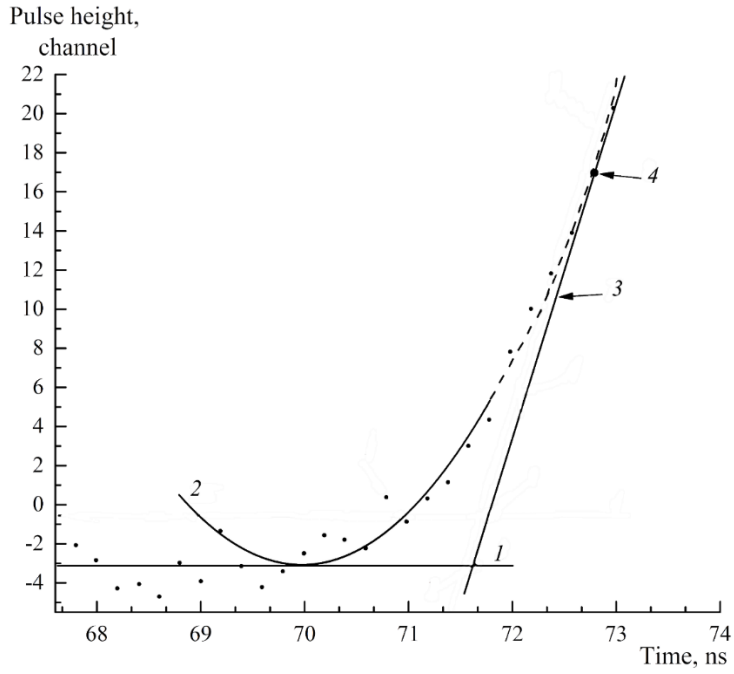

FIGURE 2. Stored waveform from the PIN diode. 1 – line corresponded to the mean value of the base-line, 2 – parabolic approximation of the initial part of the signal, 3 – linear part of the edge, 4 – sewing point.

The parabola vortex serves as a "true" timestamp. In other words, the STP algorithm allows the detection of a real point in time when the fragment hits the detector. Validation of the SPT method was performed at the time-of-flight spectrometer shown in figure 3. The fragment's TOF t_a on the segment a was measured using two microchannel plates based time detectors (MCP detectors) St1 and St2. There is no plasma delay for them, so the velocity $V_1 = a/t_a$ can be considered the true velocity of the fragment. After passing detector St2, the fragment hits the PIN diode. The velocity V_2 of the fission fragment was measured using the time stamps of the signals from the detector St2 and the PIN diode. The velocities V_1 and V_2 can be compared event by event (figure 4). It should be noted that the FF energies at the segments a and b differ by the amount of energy losses in the foil of the St2 detector (figure 3). The loss calculation was performed using the SRIM package [13], and the estimate is expected to have a systematic error. The expected calculated velocity difference is shown in figure 4 by dashed line 1. The deviation of line 1 from line 2 (dashed-dotted line in figure 4), which approximates the linear portion of the dependence $\langle V_2 - V_1 \rangle$ on V_1, does not exceed 0.01 cm·ns^{-1}, i.e. ≈1% FF's velocity. This deviation is also likely due only to a systematic error in the estimation of ΔV_c. Indeed, a priori it can be assumed that the SPT algorithm could give a systematic shift in the estimation of the TOF, but this shift should depend on the velocity of the FF to reproduce the horizontal section in the experimental graph in Fig. 4.

When the parabola approximates the initial part of the signal's edge within the SPT algorithm, the TOF (FF's velocity) or the signal amplitude are not used in any way. Thus, the very presence of a horizontal section on the graph $<V_2 - V_1> / V_1$ (figure 4) can serve as a criterion for the correctness of the sewing-parabola algorithm.

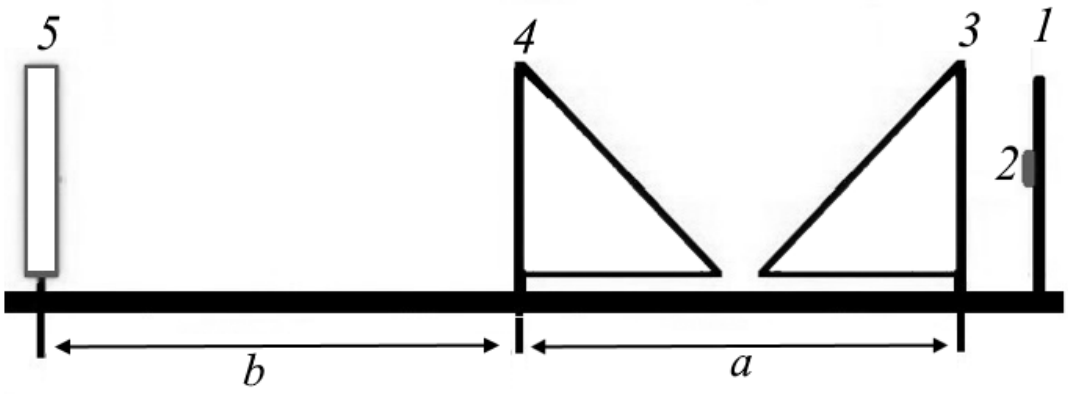

FIGURE 3. Time-of-flight spectrometer for testing SPT method using ^{252}Cf(sf) source. 1 – target holder with the ^{252}Cf(sf) source; 2, 3 – St1 micro-channel plates based timing detector; 4 – micro-channel plates based timing detector St2; 5 – PIN diode that provides the "stop" signal; flight-passes a = 14.2 cm, b = 14.1 cm.

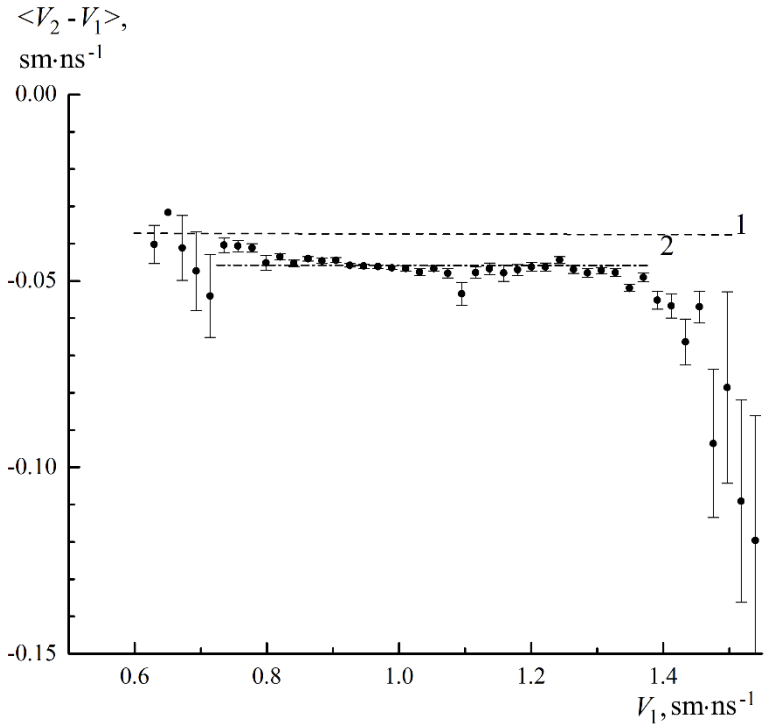

FIGURE 4. Mean difference $<V_2 - V_1>$ as a function of V_1 for the FFs from the ^{252}Cf(sf) source measured at the "*a*" and "*b*" flight segments (figure 3), respectively, as a function of V_1. The horizontal dashed line 1 corresponds to the expected calculated value $<V_2 - V_1>$, taking into account the FF energy loss in the detector St2. The horizontal dash-dotted line 2 approximates a statistically significant linear portion of the experimental dependence.

CONCLUSION

It has been analytically shown that for an arbitrary response $h(t)$ of the electronic circuit connected to the detector, the area of the output signal S remains proportional to the charge q created by the ionizing particle in the detector. The q estimation algorithm by calculating the area S of the output signal avoids the ballistic error inherent in estimating q from the amplitude of the pulse.

To increase the stability of the procedure for calculating the ion mass with respect to the errors of the input variables, the parametrization of the amplitude defect $R(M,E)$ has been modified. The significance of the introduced corrections is shown.

In a differential experiment for measuring FF's speed in ^{252}Cf (sf) by using microchannel plates based detectors and sewing-parabola time pick-off method for the signals from PIN diodes it is shown that this algorithm gives an unbiased time reference corresponding to the moment of FF detection in the detector.

ACKNOWLEDGMENTS

This work was supported by the research project № 18-32-00538 of the Russian Foundation for Basic Research (RFBR) and partially by the MEPhI Academic Excellence Project (Contract No. 02.a03.21.0005, 27.08.2013) of the Russian Science Foundation as well as by the Department of Science and Technology of the Republic of South Africa (RSA).

REFERENCES

1. D.V. Kamanin, Yu. V. Pyatkov, "Clusters in Nuclei – Vol. 3" ed. by C. Beck, Lecture Notes in Physics 875, pp. 183–246 (2013).
2. D.V. Kamanin, Yu. V. Pyatkov, Nuclear Particle Correlations and Cluster Physics Part 4. Cluster Radioactivity, Fission and SHE. World Scientific, 2017. p. 339–370.
3. Yu.V. Pyatkov et al., FIAS Interdisciplinary Science Series. Nuclear Physics: Present and Future. 2015. pp.79–88.
4. Yu.V. Pyatkov et al., Eur. Phys. J. A **45** (2010) 29–37.
5. A.O. Strekalovsky et al., Yadernaya Fizika i Inzhiniring. Vol. **6**, No. 5–6, 2015, p. 290–296 (rus).
6. Yu.V. Pyatkov et al., J. Phys.: Conf. Ser. **675** (2016) 042018.
7. Yu.V. Pyatkov et al., Bull. Russ. Acad. Sci.: Phys. **82** (2018) 804.
8. S.I. Mulgin et al., NIM A **388** (1997) 254.
9. http://edu.sernam.ru/book_sm_math2.php?id=111.
10. A.P. Tsitovich, Yadernaya elektronika. Moskva. Energoatomizdat. 1984. C. 408 (rus).
11. F. James, M. Roos, Comput. Phys. Commun. **10** (1975) 343.
12. H.W. Schmitt, W.E. Kiker, C.W. Williams, Phys. Rev. **137** (1965) B837.
13. J.F. Ziegler, M.D. Ziegler, J.P. Biersack, NIM B **268** (2010) 1818.